The effect of temperature and excitation energy of the high- and low-spin 4f→5d transitions on charging of traps in Lu_2O_3:Tb,M (M = Ti, Hf)

Kulesza, Dagmara; Bos, Adrie J.J.; Zych, Eugeniusz

DOI
10.1016/j.actamat.2022.117852

Publication date
2022

Document Version
Final published version

Published in
Acta Materialia

Acta Materialia 231 (2022) 117852

Contents lists available at ScienceDirect

Acta Materialia

journal homepage: www.elsevier.com/locate/actamat

The effect of temperature and excitation energy of the high- and low-spin 4f→5d transitions on charging of traps in Lu_2O_3:Tb,M (M = Ti, Hf)

Dagmara Kulesza[a,*], Adrie J.J. Bos[b], Eugeniusz Zych[a]

[a] Faculty of Chemistry, University of Wrocław, 14 F. Joliot-Curie Street, Wrocław 50-383, Poland
[b] Faculty of Applied Sciences, Delft University of Technology Mekelweg 15, NL 2629 JB Delft, the Netherland

ARTICLE INFO

Article history:
Received 24 June 2021
Revised 10 March 2022
Accepted 16 March 2022
Available online 22 March 2022

Keywords:
Luminescence
Defects
Thermally activated processes
Irradiation effect

ABSTRACT

This work presents a fresh insight into the excited charges trapping in the Lu_2O_3:Tb,M (M= Ti, Hf) ceramics and their characteristics as storage and/or persistent luminescence phosphors. The results were obtained by applying an exceedingly versatile set of experiments based on thermoluminescence and thermoluminescence excitation spectroscopy and exposed a dual-nature of these materials. In the contrary to the previous research, here we found that at least some of these materials can generate efficient persistent luminescence due to the presence of shallow traps which can be charged only upon specific irradiation conditions – by the spin-forbidden 4f→5d transition of Tb^{3+} around 360 nm and, possibly, the $^7F_6 \rightarrow {}^5D_3$ intra-configurational transition of the activator at just slightly longer wavelengths. Besides that, changing the sample charging temperature the efficiency of filling the traps – both deep and shallow – with the 360 nm radiation varied greatly and exposed a very broad distribution of trap energies. Charging with 360 nm radiation at room temperature fills only the shallow traps giving, never reported in Lu_2O_3:Tb,Ti and Lu_2O_3:Tb,Hf, intense persistent luminescence, while at higher temperatures the deep traps are filled. At any temperature, radiation of wavelengths < 320 nm fills almost exclusively deep traps responsible for TL at high temperatures, 230 °C in Lu_2O_3:Tb,Hf and 355 °C in Lu_2O_3:Tb,Ti.

1. Introduction

In the research on persistent luminescence and/or storage (thermoluminescence) phosphors some standard experiments are typically used to expose their main characteristics. These include studying TL glow curves after irradiation with high-energy photons (typically γ-, X- or UV-rays), fading of the TL signal, the effect of heating rate and radiation dose, and isothermal decays. Studies on evolution of charging curves [1], trap distribution [2–5], thermal ionization barrier by optical methods [6] are also exploited but are less-common in such research. They bring, however, important information and lead to better understanding of such phosphors' properties and mechanisms related to excited carriers trapping and detrapping – the core of the thermoluminescence process.

One of the least exploited research methods in this field are measurements of thermoluminescence excitation spectra (TLES). These were, however, shown to provide critical information on details of the TL mechanism in a material of interest [7]. This is a versatile, advanced technique revealing the dependence of excited carriers' behavior on the energy they acquire upon charging. Comparing TLES spectra with the steady state photoluminescence excitation ones greatly enriches knowledge and understanding of the physics of the TL process and consequently the material properties. One can find nice examples of TLES usage in studies of $M_2Si_5N_8$:Eu (M=Ca, Sr, Ba) persistent luminescence phosphor conducted by Smet et al. [8]. This method was also shown useful to establish the location of energy levels of Ce^{3+} in YAG:Ce^{3+},Yb^{3+} published by You et al. [9] and Ueda et al. [10] found the TLES spectroscopy very profitable to comprehend the mechanism of luminescence thermal quenching in singly doped YAG:Ce^{3+}. The method is time consuming and therefore it is so rarely used, despite its great usefulness.

Till now the thermoluminescence characteristics of the Lu_2O_3:Tb,M (M=Hf, Ti) co-doped storage phosphors were presented either after exposure to short-wavelength UV radiation (250–320 nm), or regular ionizing radiation, X- or β-rays [11–14]. It was shown among others that the Hf or Ti co-dopants greatly enhanced the materials energy storage capacity in comparison to their singly doped Lu_2O_3:Tb counterpart. The TL glow curves

* Corresponding author.
E-mail address: dagmara.kulesza@chem.uni.wroc.pl (D. Kulesza).

https://doi.org/10.1016/j.actamat.2022.117852

of the two compositions were characterized by a well-separated single TL peak at ∼230 °C (Tb, Hf), or ∼355 °C (Tb, Ti). The relatively deep traps giving rise to the TL of these materials combined with linear dose-response dependence over a very broad range, reaching seven-orders of magnitude make them important and interesting storage phosphors deserving still deeper understanding of their properties.

Though quite thorough, the thermoluminescent experiments presented in previous papers have not allowed for an unambiguously elucidation of the TL mechanism in the Lu_2O_3:Tb,Hf or Lu_2O_3:Tb,Ti phosphors. Some queries have yet been left open and the present paper intends to fill the gaps. On the other hand, the numerous data allowed to identify detailed doubts and questions not yet satisfactorily treated and to seek more sophisticated experimental techniques and methods to acquire complement information to grasp new insight on relevant processes occurring in these phosphors. This paper presents results of such new, advanced experiments. They indeed shed new light on these storage phosphors and broadens our understanding of their properties. We will show among others spectacular difference between TL glow curves after charging into 4f→5d allowed absorption band below ∼310 nm compared to irradiation into the analogous spin-forbidden transition [15,16] at 360 nm.

2. Experimental

2.1. Sample preparation

Details of materials' fabrication procedure was described previously [14]. Briefly, crystalline powders prepared by Pechini [17] method were cold-pressed and sintered at 1700 °C for 5 h in vacuum (Tb, Hf) or reducing gas mixture (25%H_2/75%N_2; Tb, Ti). The different atmospheres were applied as they were previously proved to give materials of better performance, though the effect of the atmosphere did not exceed a factor of 2-3 in TL efficiency. After preparation, the ceramic pellets were polished before measurements.

2.2. Measurements procedures

All powders were checked for their phase purity with X-ray diffraction (XRD) technique using a Bruker D8 Advance diffractometer equipped with a Cu lamp and its Kα1 = 1.54433 Å radiation. The TL measurements were performed with a Risø TL/OSL reader model DA-15 and a controller model DA-20 with heating rate of 5 °C/s. Excitation was executed with UV radiation from a Xe lamp. The TL excitation spectra (TLES) measurements consisted of three parts: (1) irradiation of the sample with the desired wavelength, (2) measurement of the TL glow curve and (3) integration of the TL glow curve intensity at the desired temperature range. This sequence was repeated for excitation wavelengths between 225 and 500 nm and the integrated TL, corrected for the difference in number of incident photons, plotted as a function of the excitation wavelength. More details can be found in [7]. The series TL excitation spectra (TLES) measurements for Lu_2O_3:Tb,Ti material were recorded also in wide range of sample temperatures during irradiation at a certain wavelength. In the given experiment the sample was cooled down to room temperature after previous illumination at the charging temperature and then the TL curve was recorded. Photoluminescence excitation spectra (PLES) were recorded using FLS 980 spectrofluorometer from Edinburgh Instruments using a 450 W Xenon arc lamp as an excitation source. The spectra were collected monitoring at 542 nm ($Tb(C_{3i})$) and 480 nm ($Tb(C_2)$) luminescence [18].

Persistent luminescence of Lu_2O_3:Tb,Hf and Lu_2O_3:Tb,Ti after 2 min excitation with 360 nm or 270 nm wavelength was detected using an EMI 9635 QA photomultiplier tube (PMT) over 20 min.

3. Results

3.1. Thermoluminescence excitation spectra

The efficiency of traps filling on charging radiation wavelength (energy) has been investigated by measuring the TLES for both compositions. The results are presented in Fig. 1a. Two wavelength ranges can be distinguished in the spectra. The first structured band is located in the 250–330 nm range and is composed of two overlapping components. They correspond to the 4f→5d PL excitation transitions of $Tb(C_2)$ (∼270 nm) and $Tb(C_{3i})$ (∼310 nm) as shown in Fig. 1b presenting PLES of Lu_2O_3:Tb,Hf and reported and thoroughly analyzed in literature [14]. For the (Tb, Ti) composition the PLES are very similar to (Tb, Hf) and are not presented.

Charging the co-doped materials with the 250–330 nm radiation leads to a strong TL with maxima dependent on the co-dopant, as seen in Fig. 1c. The most intense TL of the (Tb, Hf) ceramic is at 230 °C, while for the (Tb, Ti) it comes at 355 °C. Note that in both compositions there is also a low-temperature low-intensity TL peak, somewhere around 90–110 °C. However, upon such charging (< 330 nm), their relative intensities are quite low, especially for the (Tb, Ti) co-doped sample. Very similar glow curves were recorded after charging the ceramics with X- or β-rays, hence when the liberated charge is delocalized [19].

A different situation is observed for single-doped Lu_2O_3:Tb as seen in Fig. 1c. After charging with UV radiation of wavelengths shorter than ∼330 nm, the maximum of the TL curve is located around 80 °C. Some very weak satellite TL peaks are spread over a wide range of higher temperatures. The intensity of the presented TL curves in Fig. 1c is normalized, thus it is noteworthy that the absolute TL of the single-doped ceramic is much weaker compared to the TL of the co-doped materials.

Unexpected differences between the TLES spectra of the co-doped samples are seen around 360 nm, see Fig. 1a. This feature is related to the 4f→5d spin-forbidden transition of Tb^{3+} [15]. Only for the (Tb, Ti) ceramics this TL excitation band intensity is comparable with the 4f→5d bands <330 nm representing the allowed 4f→5d transitions. Fig. 1d shows the normalized TL glow curves of the singly doped (Tb) and both co-doped materials after irradiation into the 360 nm 4f→5d spin-forbidden band. Their shapes are now practically identical with a common maximum at 80 °C. Clearly, the TL originates from the same type of defect in all compositions. This implicates that this TL is unrelated to co-dopant ions but rather associated with an intrinsic defect. Comparing the results presented in Fig. 1c (charging at 304 nm by means of the allowed 4f→5d transition) and in Fig. 1d (charging at 360 nm through the spin-forbidden 4f→5d) it is obvious that we have two entirely different (set of) traps and different ways of filling them.

The 360 nm charging radiation does not carry enough energy to raise the electron all the way up to the host conduction band at room temperature [20]. Thereby, the shallow traps giving TL at 80 °C have to be filled through a local, tunneling-type process. In contrary, the 304 nm radiation is expected to raise the electron close enough to the conduction band to allow it to escape the Tb^{3+} ion. Then, the free electron migrating through the CB over some distance can fall into the deeper trap(s) responsible for the higher-temperature TL.

3.2. Persistent luminescence decay

Giving that two of the samples, (Tb, Hf) and (Tb, Ti), exhibited significant, green afterglow after charging with the 360 nm

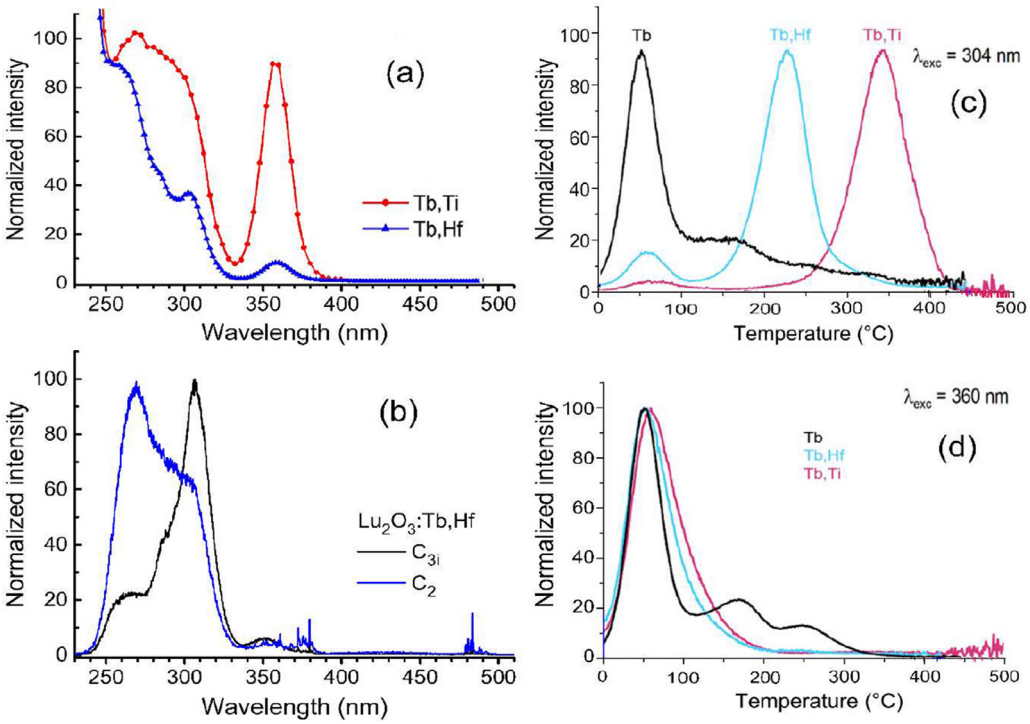

Fig. 1. (a) Thermoluminescence excitation spectra of Lu_2O_3:Tb,M (M= Hf, Ti). (b) Photoluminescence excitation spectra of Lu_2O_3:Tb,Hf monitored at emission peak wavelength coming from two different Tb^{3+} site positions in Lu_2O_3. (c,d) Normalized TL glow curves of Lu_2O_3:Tb and Lu_2O_3:Tb,M (M= Hf, Ti) after excitation with λ = 304 nm (c) and λ = 360 nm (d) (heating rate 5 °C /s).

radiation we performed more detailed investigation of this effect in these materials. The persistent luminescence decay curves recorded after charging at 360 nm and 270 nm are compared in Fig. 2a,b. After the latter irradiation the afterglow emission is very weak and in the (Tb, Ti) material it is almost absent since the constant signal shown is at background level.

In the contrary, after charging at 360 nm both materials show intense PersL, as expected from their TLs presented in Fig. 1d. Hence, after such charging, these ceramics become regular green persistent luminescence phosphors. The PersL decays faster in the (Tb, Hf) ceramic than in the (Tb, Ti) one. This may result simply from a higher concentration of the filled traps in the (Tb, Ti) material than in the (Tb, Hf) one. This is reasonable considering the difference in their TLES presented in Fig. 1a. This is the (Tb, Ti) ceramic which presents the very strong TL excitation band around 360 nm, while in the (Tb, Hf) phosphor this feature is much lesser. This makes it reasonable to expect that traps filling is much more effective in Lu_2O_3:Tb,Ti than in Lu_2O_3:Tb,Hf.

The above observations are in line with the glow curves (Fig. 2c,d) recorded for both materials after 20 min decay measurements (Fig. 2a,b). It is striking that the (Tb, Ti) glow curve presents still very intense TL peak at 110 °C implying that its PersL could still continue for a long time. Note that the peak is well shifted now to higher temperature compared to what was seen taking such a measurement right after the charging (see Fig. 1d). This indicates that the low-temperature TL peak results from at least two superimposed components. For (Tb, Ti) sample, the TL glow curve after irradiation at 270 nm contains only less intense peak at 355 °C after the 20 min delay (Fig. 2c). In the case of the (Tb, Hf) phosphor after the 20 min delay both TL glow curves show low-intensity TL around 100 °C. 20 min after the 270 nm charging of this material a strong component at 270 °C dominates the TL (Fig. 2d). These data show that especially efficient PersL is observed from the Lu_2O_3:Tb,Ti ceramic when 360 nm charging radiation is employed. This occurs as this phosphor benefits of the very effective low-temperature traps filling by means of the Tb^{3+} 4f→5d spin-forbidden transition, see Fig. 1a.

Fig. 3 shows the inverse of the PersL intensity (I) decay after the 360 nm irradiation of the (Tb, Ti) and (Tb, Hf) ceramics. For each sample the I^{-1} vs. time dependence is essentially linear. This can be explained twofold, resulting either from tunneling [21] or from distribution of trap energies [22,23]. We will later see that in the case of the ~100 °C peak both are true.

For a deeper understanding of the trapping mechanism the influence of the charging temperature on the traps filling was evaluated. Being a time-consuming experiment, it is rarely used in such research, but it can bring important information on the system under investigation. In this experiment we limited ourselves to just one composition, Lu_2O_3:Tb,Ti, owing to its highest PersL intensity.

3.3. Temperature dependence of trap filling and thermal activation energy determination

Increasing the temperature during the sample irradiation with particular wavelength can bring information about selective filling of the traps [8], ionization energy (the energy separation between the excited state of the luminescence center and the bottom of the host CB [24]), thermal quenching processes [25] as well as trap energy distribution and thermal barrier for charging [4]. Six different charging wavelengths have been utilized. Part of them correspond with the 4f→5d spin-allowed Tb^{3+} absorption (270, 287, 304, 316), 360 nm represents the spin forbidden 4f→5d transition and the 332 nm locates exactly between these two. Below three representative cases (270, 316, and 360 nm irradiation) are discussed (see Figs. 4a,c and 5 respectively). Based on these results and using Arrhenius plots (Fig. 4b,d), activation energy of the thermal ionization of the relative 5d excited state of Tb^{3+} for every charging wavelengths were calculated. In Fig. S1 results for the other charging wavelengths are presented.

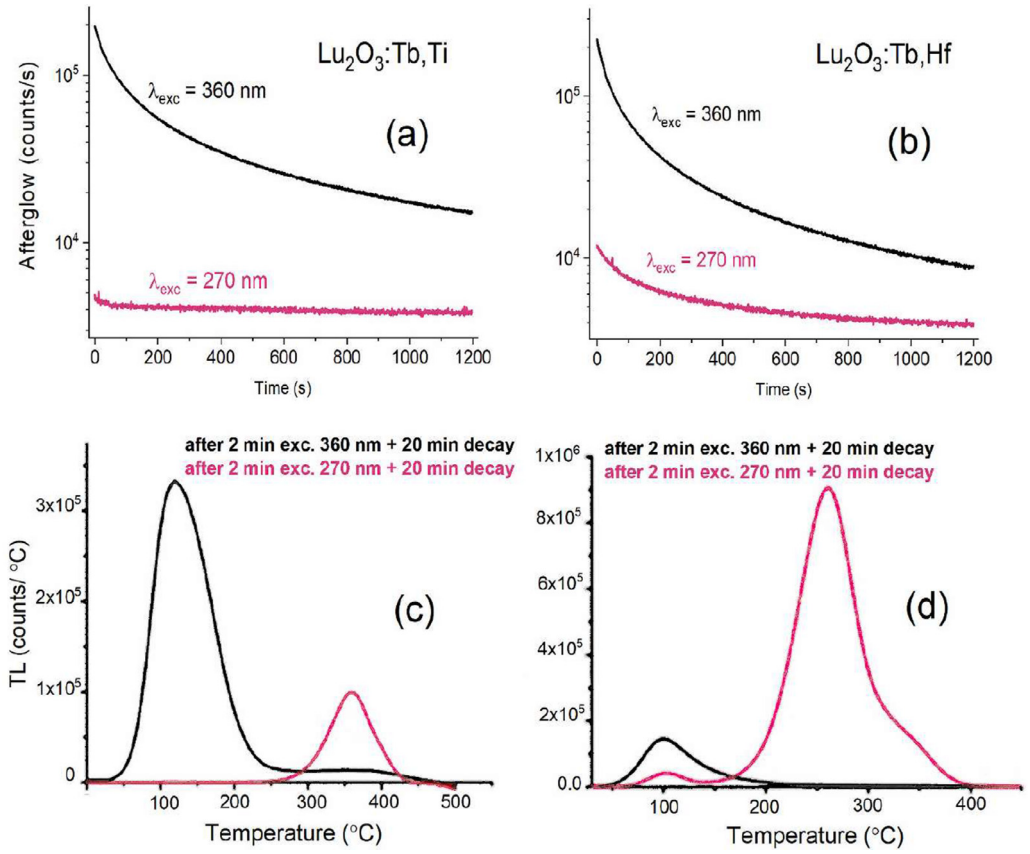

Fig. 2. Persistent luminescence from Lu_2O_3:Tb,Ti (a) and Lu_2O_3:Tb,Hf (b) recorded for 20 min after 2 min excitation in the $[HS]5d_1$ band (360 nm) and $[LS]5d_1$ band (270 nm). Glow curves of Lu_2O_3:Tb,Ti (c) and Lu_2O_3:Tb,Hf (d) after 2 min excitation with two different wavelengths and 20 min decay (heating rate 5 °C /s).

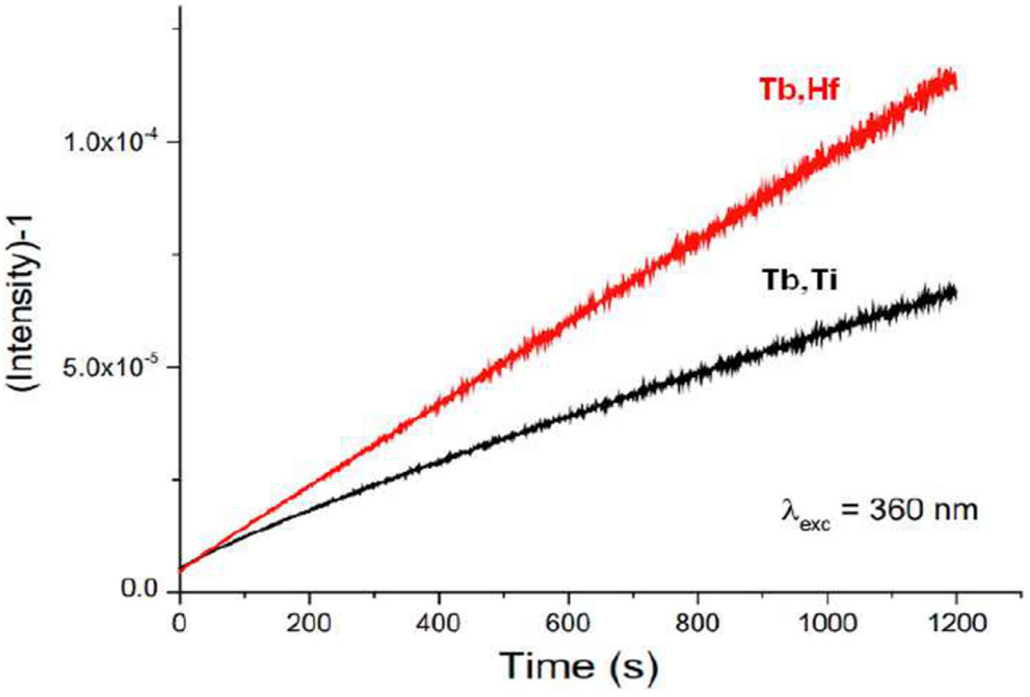

Fig. 3. Inverse of the Persistent Luminescence after excitation with 360 nm as function of time showing a 1/t behavior (data of Fig. 2a,b).

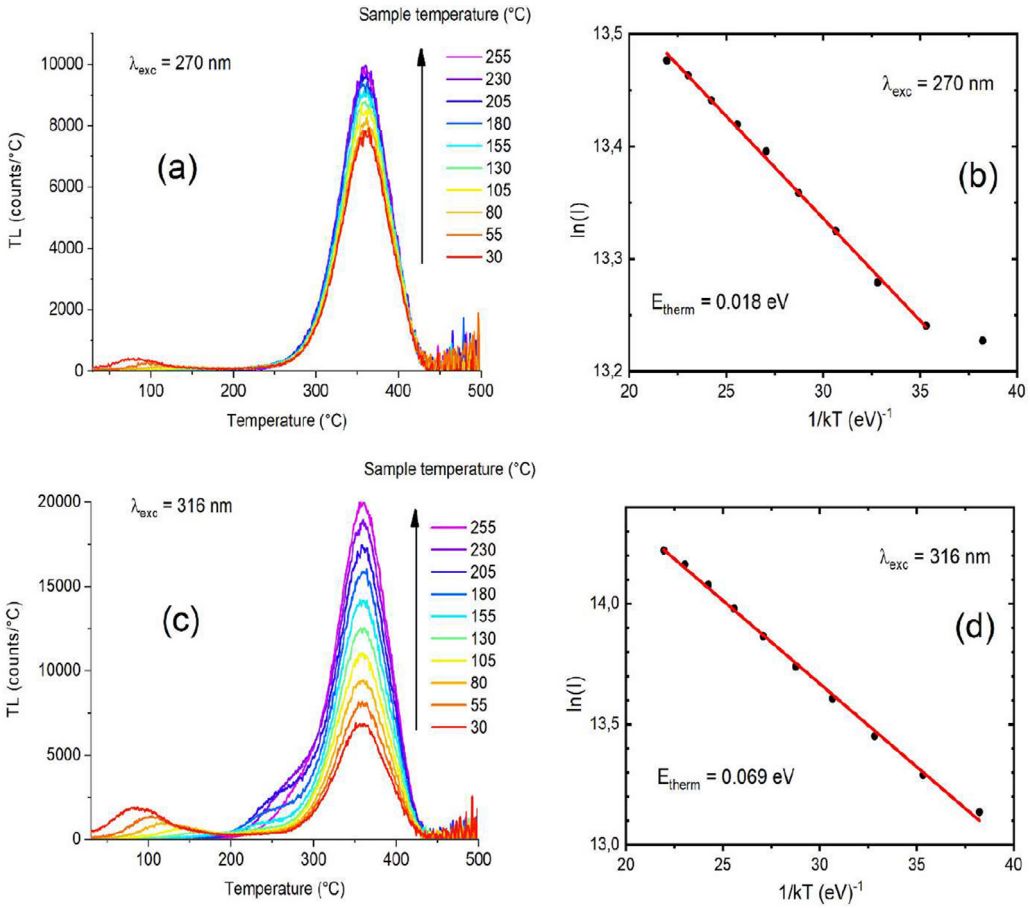

Fig. 4. On the left: Glow curves of Lu_2O_3:Tb,Ti measured after irradiation with a 270 nm (a) and 316 nm (c) wavelength, λ_{exc}, and the sample at a certain temperature (heating rate 5 °C /s). On the right: Arrhenius plots (b, d).

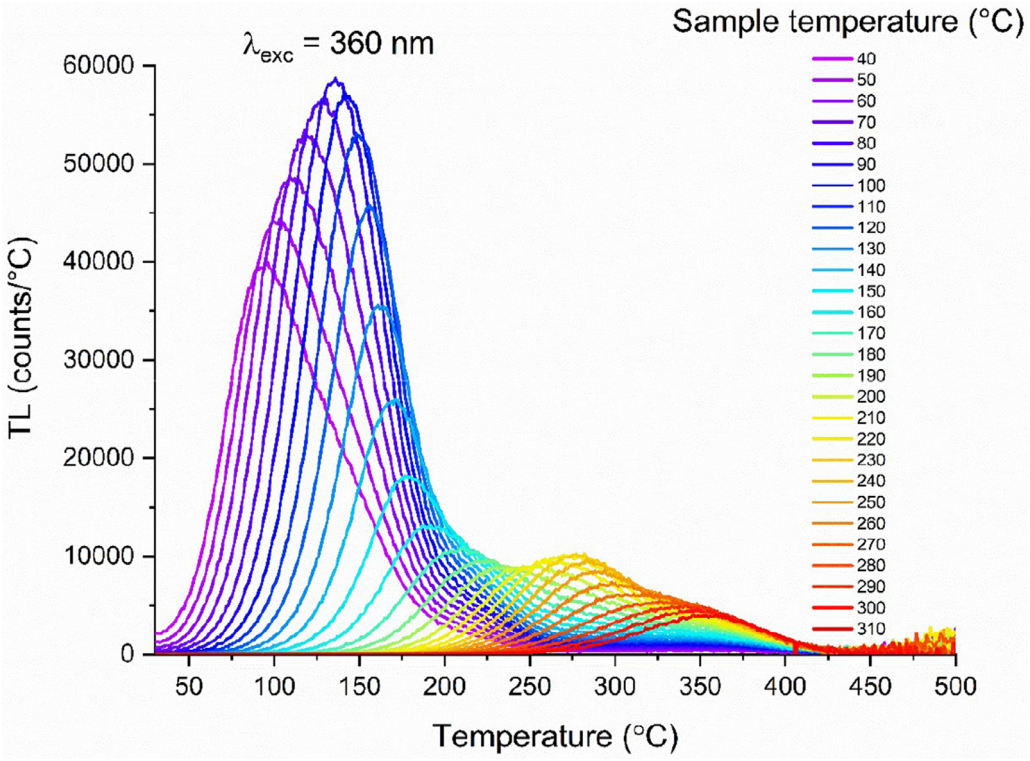

Fig. 5. Glow curves of Lu_2O_3:Tb,Ti measured after irradiation with 360 nm wavelength at a specified temperature (heating rate 5 °C/s).

The glow curves collected for charging at 270 nm are presented in Fig. 4a. As the charging temperature increases, the intensity of the main peak at 360 °C also increases altogether by about 20%. This indicates that trap filling process is thermally activated [3] although the effect of thermal energy is not very potent. Similar result was observed by Fasoli et al. in $Lu_2Si_2O_7$:Pr^{3+} [6] and in Eu-doped nitridosilicates studied by Smet et al. [8].

Upon charging with 316 nm a comparable effect is observed but it is much more profound now (Fig. 4c). The TL intensity increases by a factor of ~3 when the temperature increases from 30 to 255 °C. Clearly, the thermal energy has a huge impact on the charging efficiency at the 316 nm. An opposite result is seen for the low-intensity TL peak with maximum at 80–100 °C. With the increase of the irradiation temperature not only its intensity decreases but also its maximum shifts continuously to higher temperature. Both effects indicate the presence of a continuous distribution of trap depth energies. When higher thermal energy is available the shallowest traps are immediately bleached and only the deeper fraction of the distribution continuous to store the carriers.

These experiments revealed yet another trapping center giving TL peak around 250 °C. It overlaps partly with the most intense TL band at 355 °C. Up to the charging temperature of 155 °C this trap does not get filled. Only above this temperature its charging becomes effective. Hence, the trap at 250 °C is also fed by means of a thermally-activated process. Since it does not trap any carriers at lower temperatures it is plausible to expect that it gains energy from the deepest trap giving TL at 355 °C. Such an energy/electrons exchange may occur when an *excited state* of the deeper trap (355 °C) is in resonance with the shallower one (250 °C) as described in [26].

The usage of the 360 nm radiation for charging, i.e. exploiting the spin-forbidden 4f→5d transition of Tb^{3+} at different temperatures, leads to tremendous and complex changes in the glow curves, see Fig. 5. As the charging temperature increases, the maximum of the glow curve shifts continuously from 80 °C to 355 °C indicating a profound effect of thermal activation on the traps filling. Altogether, three TL components can be easily distinguished and each of them shows trap depths distribution.

The intensity of the glow dominant peak at 95 °C increases by about 50% until charging temperature reaches 90 °C. This indicates adequately more carriers trapped in the sample. Upon further increase of the irradiation temperature the TL peak continues shifting towards higher temperatures though the TL intensity decreases. Intriguingly, when the charging temperatures is higher than ~140 °C even deep traps responsible for TL peaks in the range ~200–355 °C get filled and contribute to TL. Hence, even the deepest traps can be filled using the 360 nm radiation if sufficient thermal energy is accessible to attain synergy of optical photons and thermal phonons.

For the singly doped Lu_2O_3:Tb TL glow curves upon charging at room temperature with 300 and 360 nm radiation are compared in Fig. S4. Their shape is perfectly the same with the main TL peak around 80 °C. Yet, the TL intensity is greatly larger upon the 360 nm charging. This difference we will address in the Discussion section.

Based on the presented Arrhenius plots (Figs. 4b,d and S1) thermal activation energy, E_{therm}, for the particular charging wavelength could be calculated. An impressive correlation of the TLES and E_{therm} in showed in Fig. 6. Note that the E_{therm} is shown as a negative value i.e. the extra energy needed to release an electron into the CB after its elevation to a specific 5d level of Tb^{3+} ion in the Lu_2O_3 host. The perfect correlation (between red and blue curves) shows that the energy gap between the ground state of Tb^{3+} and the bottom of the CB corresponds with ~3.9 eV (~320 nm).

4. Discussion

Both the previously published literature and the data presented in this paper show that the co-dopants, Hf and Ti introduce specific deep traps giving rise to TL at high temperatures, above 200 °C. The present research proves that these traps may be filled with high-energy UV radiation of $\lambda < 320$ nm. However, efficiency of such charging shows a characteristic temperature dependence. The temperature effect becomes more profound when the charging energy increases (the wavelength shortens). This is understandable on the bases of the Dorenbos VRBE diagram which proves that the $\lambda < 320$ nm radiation raises electrons to 5d levels close to but still below the host CB. The thermal energy allows coupling of the excited electron with the delocalized states of CB. Then, the free carrier finds its deep trap.

Yet, an extreme case of temperature effect on traps charging is clearly visible when the irradiation exploits the 4f→5d spin-forbidden transition at 360 nm (Fig. 5). At room temperature it fills only shallow traps giving TL at 80 °C. Then, when the temperature increases, continuously deeper traps get filled and consequently TL appears at accordingly higher temperatures. Finally, when the irradiation temperature is 210–310 °C the deepest traps are filled and the TL peaks at ~260–355 °C. This makes the Lu_2O_3:Tb,Ti TL phosphor a kind of temperature sensor. This would be a brand-new approach to temperature reading by means of a temperature-dependent (thermo)luminescence property. Any deeper analysis of this suggestion is beyond the scope of this paper and will be a subject of our future research.

Efficient filling of the shallow traps upon charging with 360 nm radiation at room temperature (or close to it) gives rise to strong persistent luminescence of Lu_2O_3:Tb,Ti (as well as Lu_2O_3:Tb,Hf, which is, however, less potent). The set of the glow curves presented at Fig. 5 and analysis presented in Figs. S2 and S3 allow to estimate that the low-temperature TL is associated with the distribution of trap depths about 0.8 eV. Then, the distribution of the energy of the deepest traps, giving TL around 355 °C, is associated with trap depths of about 1.87 eV. These data were used to construct the diagram presented in Fig. 7. For clarity the figure does not contain data for both sites of Tb^{3+} in Lu_2O_3 (see the Introduction). Their 5d levels are not that much different in energy, see the excitation spectra on Fig. 1. From Fig. S2b it also appears that no semi-localized transitions take place in the Lu_2O_3:Tb,Ti ceramics, while in the Lu_2O_3:Pr,Ti such mechanism was evidently proved [27].

Based on the data presented in the Supplementary Materials file (Table S1 and Fig. S5) and the Dorenbos' VRBE model [28–31] a complete energy level diagram of the Lu_2O_3:Tb,Ti ceramic can be proposed, see Fig. 7. The position of the ground state of the Tb^{3+} (~ -6.8 eV) is found using the Dorenbos approach but is also confirmed by results presented in Fig. 6. Its location implies that Tb^{3+} can act as a deep hole trap and this agrees with previous studies [12].

The scheme in Fig. 7 shows that the energy of the shallow trap(s) matches perfectly the energy position of the 5d (spin-forbidden – 360 nm) level of Tb^{3+}. Tunneling requires overlapping of the donor and acceptor's wavefunctions of the levels of interest. Then, supposedly, it is more probable between the 5d level of Tb^{3+} around 360 nm and the shallow trap state than between the (screened) 4f levels of Tb^{3+} and the trap. Yet, some contribution to the tunneling also from the 4f $^5D_3$ levels of Tb^{3+} cannot be discarded and in fact is quite probable. As seen in Figs. 1b and 7, energetically the Stark levels of the $^5D_3$ state are quite suitably positioned for the discussed tunneling. Hence, both the $^5D_3$ levels of Tb^{3+} and its 5d forbidden level are expected to be engaged in filling the shallow traps or receiving energy from them. At higher

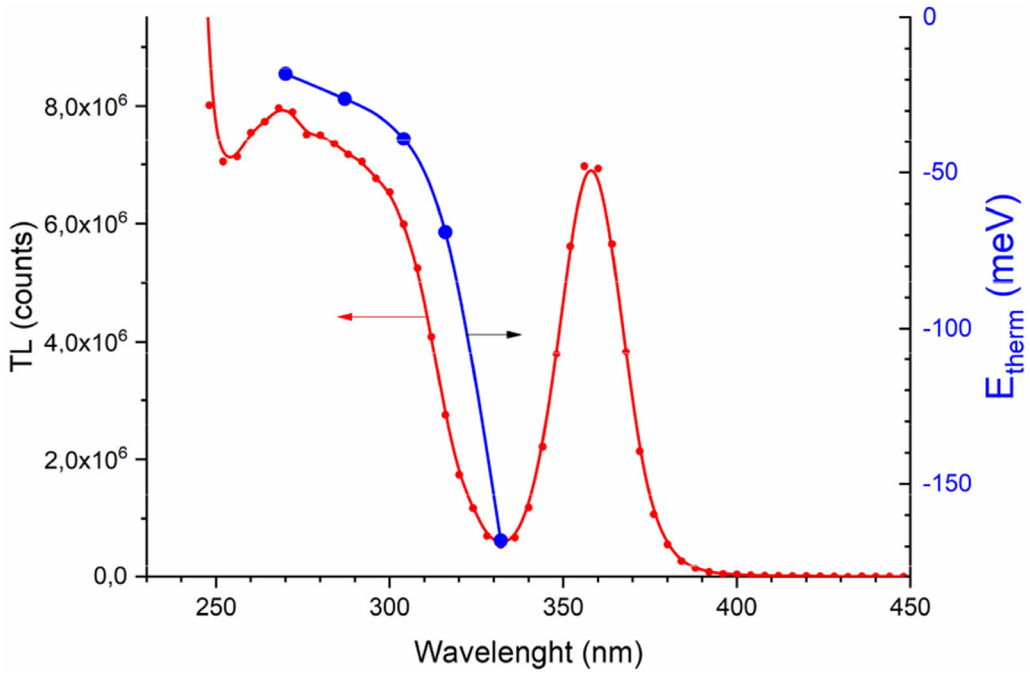

Fig. 6. TL excitation spectrum of Lu_2O_3:Tb,Ti together with the thermal activation energy derived from the Arrhenius plots depicted as a function of the excitation wavelength.

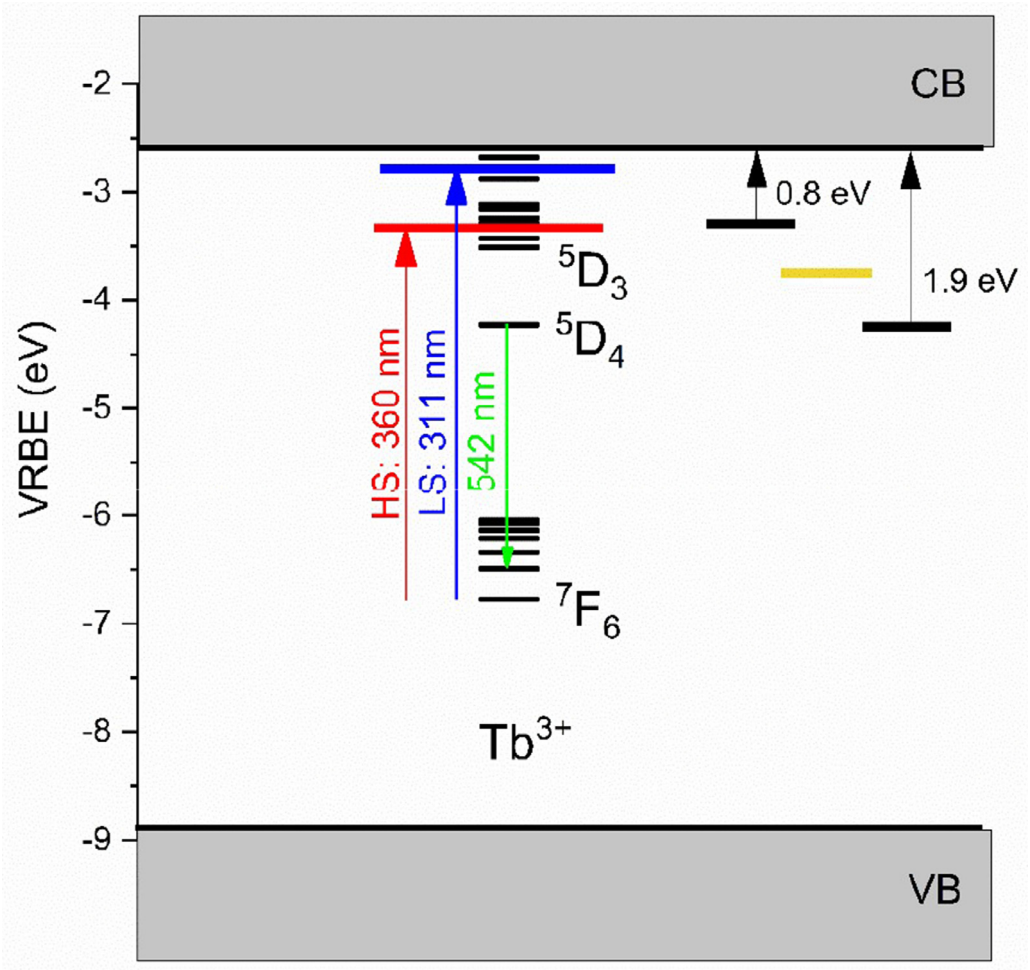

Fig. 7. Vacuum-referred binding energy (VRBE) diagram of Lu_2O_3:Tb,Ti showing the energies of the 4f ground state of Tb^{3+} and LS and HS 4f→5d transition as well as CB and VB of the Lu_2O_3 host. Thermal trap depths (black lines) were estimated from glow curves (see Figs. S2 and S3) and the yellow line represents the medium-energy trap whose depth was roughly approximated. (For interpretation of the references to colour in this figure legend, the reader is referred to the web version of this article.)

temperatures the involvement of the $^5D_3$ levels should even increase.

Since the $^5D_3$ is located slightly below the HS 360 nm forbidden transition, it might be considered useful to fill the deep traps either by tunneling or by thermal stimulation. The latter would easily involve the HS state (360 nm, Fig. 7) and thus would rather lead to the tunneling towards the shallow trap, as just discussed. The former mechanism – tunneling from the $^5D_3$ to the deeper traps - cannot be excluded, at first. Yet, its efficiency would need a spatial proximity of both interacting entities (Tb^{3+} and the trap) especially that the shielded 4f levels hardly interact even with the ligands from their first coordination sphere. Hence, one should not expect it plays any significant role in the discussed TL processes.

The presented scheme perfectly accords with the results. For shorter wavelengths (< 320 nm, LS 4f→5d band transition) the charging energy is high enough to ionize Tb^{3+}, with just small help of thermal phonons easily available at room temperature, and release the electron into the CB. From there, mostly the high-temperature traps are filled (in both co-doped samples) while the shallower ones contribute to TL only moderately. The extra thermal energy, E_{therm}, needed to promote the electron to CB is quantitatively revealed in the Arrhenius plots (Figs. 4b,d and S1). It increases continuously with decreasing energy of the charging photons, as expected. Note that upon 316 and 332 nm radiation additional medium trap is exposed (yellow line in the scheme in Fig. 7) in TL glow curves (∼250 °C) populated only in a specific range of charging temperature, namely 155–255 °C. The energy is supposed to come from the deepest trap.

The usage of the 360 nm excitation (into HS 4f→5d band) produces the low-temperature glow peak leading to persistent luminescence. Since this excitation energy is not able to cause the Tb^{3+} ionization at room temperature it is implied that these shallow traps are filled by a tunneling-type local process. As a result, the room temperature persistent luminescence decay shows the 1 over *t* behavior. All that agrees perfectly also with lack of conductivity upon the 360 nm irradiation showed previously in the Lu_2O_3:Tb,Hf sample [20].

The intriguing gradual change of the glow curves under 360 nm excitation when sample temperature is continuously raised proves that whole complex trapping sites form in fact a continues distribution of trapping centers. Then the higher-temperature glow peaks cannot be related one-to-one to the co-dopants. The co-activators definitely enhance the population of the traps naturally occurring in the host.

Finally, we want to deal with the observed greatly preferential filling of the deeper traps compared to charging of the shallow ones (giving TL below ∼100 °C) with high-energy radiation (< 320 nm). In general, it means that electrons which happened to get excited to the conduction band and gained the possibility of moving over some distances there are prone to fall into the deeper traps favorably. This means that the free electrons (those from the conduction band) capturing cross section of the deep traps [32–34] is much larger than the trapping cross section of the shallow traps. It is noteworthy that there are no signs of any energy (excited electrons) exchange between the two types of traps at least around room temperature. Hence, this is indeed the probability of capturing the free electrons, which differs the two types of the trapping sites.

It was previously concluded that the deep traps in Lu_2O_3:Tb,Hf and Lu_2O_3:Tb,Ti represent the charge transfer $O^{2-}\rightarrow Ti^{4+}/Hf^{4+}$ states [14,18,20]. The co-dopants offer empty orbitals where the electron may locate forming such an entity. Since, by its very nature, it is strongly spatially spread it may especially effectively interact with the free electron from the conduction band. This is even facilitated by the extra positive charge of the $Hf^{\bullet}_{Lu}$ or $Ti^{\bullet}_{Lu}$ defects. The origin of the shallow electron trap is not clear. In Lu_2O_3:Tb,M (M = Ca, Sr, Ba) with similarly positioned TL around 100 °C it was postulated to be associated with anionic vacancy sites in [35]. Yet, in those ceramics, it could be easily effectively charged with the wavelengths shorter than ∼320 nm, which is in contrast with Lu_2O_3:Tb (see Fig. S4). Hence, the intrinsic defects in the singly doped Lu_2O_3:Tb have to have different origin. Advanced EPR spectroscopy might shed more light on this. Nevertheless, it is clear that the competition for the free electrons in CB is won by the $Hf^{\bullet}_{Lu}$ or $Ti^{\bullet}_{Lu}$ defects. Note that the above reasoning is perfectly in line with the TL results for the singly doped Lu_2O_3:Tb in which the glow curves after charging with 300 nm and 360 nm radiation are practically identical in shape and possess only the low temperature TL coming from the shallow traps but only upon the 360 nm charging the TL is intense (Fig. S4).

5. Conclusions

In-depth research of Lu_2O_3:Tb,M (M= Ti, Hf) sintered ceramics' thermoluminescent properties was conducted and synergy offered by combining TLES and PLES spectroscopy at different temperatures and a set of TL advanced measurements was successfully used to disclose new characteristics of these phosphors. It was proved that charging energy may greatly affect TL properties of the materials leading to persistent luminescence after ∼360 nm irradiation or permanent charge carrier's storage after exposure to shorter wavelengths. The systematic research on the effect of the sample temperature on charging the traps using photons of specific energies revealed the possibility of selective filling the various trapping sites in the investigated materials Furthermore, the combined effect of thermal phonons and optical photons allowed a precise positioning of the 5d levels of Tb^{3+}, both HS and LS, within the energy bandgap. Lu_2O_3:Tb,Ti shows intense persistent luminescence after excitation into the spin forbidden 4f→5d (HS) absorption band and the electron trapping and detrapping proceed via a localized tunneling-like transition. Another unique TL features of Lu_2O_3:Tb,Ti is its extremely broad range of continuous distribution of trap depths. This could be observed only upon charging with the 360 nm radiation when assisted with thermal phonons. This, in turn, allows us to consider this ceramic as a possible temperature sensor. It will, obviously, need a focused research with precisely and deliberately defined experiments specific to this field. Nevertheless, directly from the glow curve position and shape, the material might obviously sense the temperature of its charging. Also, the afterglow intensity and its decay kinetics measured at specific (for example room) temperature should be strongly dependent on the temperature of the sample previous charging. One can imaging specific application of such effects. Bill Yen, once said about persistent luminescent phosphors: "This is our imagination, which limits their applications".

Declaration of Competing Interest

The authors declare that they have no known competing financial interests or personal relationships that could have appeared to influence the work reported in this paper.

Acknowledgments

Financial support by the Polish National Science Centre (NCN) under the grant OPUS #UMO-2017/25/B/ST5/00824 is gratefully acknowledged. Research project partly supported by program "Excellence Initiative – Research University" (IDUB) for years 2020-2026 for University of Wrocław (grant # BPIDUB.4610.21.2021.KP.B).

Supplementary materials

Supplementary material associated with this article can be found, in the online version, at doi:10.1016/j.actamat.2022.117852.

References

[1] C. Tydtgat, K.W. Meert, D. Poelman, P.F. Smet, Optically stimulated detrapping during charging of persistent phosphors, Opt. Mater. Express 6 (2016) 844, doi:10.1364/ome.6.000844.

[2] J.T. Randall, M.H.F. Wilkins, Phosphorescence and electron traps. I. The study of trap distributions, Proc. R. Soc. Lond. Ser. A Math. Phys. Sci. 184 (1945) 365LP–389 http://rspa.royalsocietypublishing.org/content/184/999/365.abstract .

[3] K. Van Den Eeckhout, A.J.J. Bos, D. Poelman, P.F. Smet, Revealing trap depth distributions in persistent phosphors, Phys. Rev. B Condens. Matter Mater. Phys. 87 (2013) 1–11, doi:10.1103/PhysRevB.87.045126.

[4] A. Feng, J.J. Joos, J. Du, P.F. Smet, Extracting trap depth distributions in persistent phosphors with a thermal barrier for charging, Phys. Rev. B (2022) Accepted 25 January, available on-line at arXiv preprint arXiv:2012.11300.

[5] J. Du, A. Feng, D. Poelman, Temperature dependency of trap-controlled persistent luminescence, Laser Photonics Rev. 14 (2020) 1–9, doi:10.1002/lpor.202000060.

[6] M. Fasoli, A. Vedda, E. Mihóková, M. Nikl, Optical methods for the evaluation of the thermal ionization barrier of lanthanide excited states in luminescent materials, Phys. Rev. B Condens. Matter Mater. Phys. 85 (2012) 1–8, doi:10.1103/PhysRevB.85.085127.

[7] A.J.J. Bos, R.M. Van Duijvenvoorde, E. Van Der Kolk, W. Drozdowski, P. Dorenbos, Thermoluminescence excitation spectroscopy : a versatile technique to study persistent luminescence phosphors, J. Lumin. 131 (2011) 1465–1471, doi:10.1016/j.jlumin.2011.03.033.

[8] P.F. Smet, K. Van Den Eeckhout, A.J.J. Bos, E. Van Der Kolk, P. Dorenbos, Temperature and wavelength dependent trap filling in $M_2Si_5N_8$:Eu (M=Ca, Sr, Ba) persistent phosphors, J. Lumin. 132 (2012) 682–689, doi:10.1016/j.jlumin.2011.10.022.

[9] F. You, A.J.J. Bos, Q. Shi, S. Huang, P. Dorenbos, Electron transfer process between Ce^{3+} donor and Yb^{3+} acceptor levels in the bandgap of $Y_3Al_5O_{12}$ (YAG), J. Phys. Condens. Matter 23 (2011), doi:10.1088/0953-8984/23/21/215502.

[10] J. Ueda, P. Dorenbos, A.J.J. Bos, A. Meijerink, S. Tanabe, Insight into the thermal quenching mechanism for $Y_3Al_5O_{12}$:Ce^{3+}through Thermoluminescence Excitation Spectroscopy, J. Phys. Chem. C 119 (2015) 25003–25008, doi:10.1021/acs.jpcc.5b08828.

[11] D. Kulesza, J. Trojan-Piegza, E. Zych, Lu_2O_3:Tb,Hf storage phosphor, Radiat. Meas. 45 (2010) 490–492, doi:10.1016/j.radmeas.2009.12.008.

[12] D. Kulesza, E. Zych, Managing the properties of Lu_2O_3 :Tb,Hf storage phosphor by means of fabrication conditions, J. Phys. Chem. C 117 (2013) 26921–26928, doi:10.1021/jp410313w.

[13] D. Kulesza, A. Wiatrowska, J. Trojan-Piegza, T. Felbeck, R. Geduhn, P. Motzek, E. Zych, U. Kynast, The bright side of defects: chemistry and physics of persistent and storage phosphors, J. Lumin. 133 (2013) 51–56.

[14] D. Kulesza, P. Bolek, A.J.J. Bos, E. Zych, Lu_2O_3-based storage phosphors. An (in)harmonious family, Coord. Chem. Rev. 325 (2016) 29–40, doi:10.1016/j.ccr.2016.05.006.

[15] R.T. Wegh, A. Meijerink, Spin-allowed and spin-forbidden 4fn ↔ 4fn-1 5d transitions for heavy lanthanides in fluoride hosts, Phys. Rev. B Condens. Matter Mater. Phys. 60 (1999) 10820–10830, doi:10.1103/PhysRevB.60.10820.

[16] L. Van Pieterson, M.F. Reid, G.W. Burdick, A. Meijerink, 4fn - 4fn-1 5d transitions of the heavy lanthanides: experiment and theory, Phys. Rev. B Condens. Matter Mater. Phys. 65 (2002) 1–13, doi:10.1103/PhysRevB.65.045114.

[17] M.P. Pechini, Method of preparing lead and alkaline earth titanates and niobates and coating method using the same to form a capacitor, US Pat 3330697 (1967).

[18] M. Sójka, D. Kulesza, P. Bolek, J. Trojan-Piegza, E. Zych, Tracing mechanism of optically and thermally stimulated luminescence in Lu_2O_3:Tb,M (M = Hf, Zr, Ti) ceramic storage phosphors, J. Rare Earths 37 (2019) 1170–1175, doi:10.1016/j.jre.2018.12.012.

[19] D. Kulesza, A.J.J. Bos, E. Zych, On energy storage of Lu_2O_3:Tb,M (M=Hf, Ti, Nb) sintered ceramics: glow curves, dose-response dependence, radiation hardness and self-dose effect, J. Alloy. Compd. 769 (2018) 794–800, doi:10.1016/j.jallcom.2018.07.360.

[20] N. Majewska, T. Lesniewski, S. Mahlik, M. Grinberg, D. Kulesza, J. Ueda, E. Zych, Properties of charge carrier traps in Lu_2O_3 :Tb,Hf ceramic storage phosphors observed by high-pressure spectroscopy and photoconductivity, J. Phys. Chem. C (2020), doi:10.1021/acs.jpcc.0c04056.

[21] P. Avouris, T.N. Morgan, A tunneling model for the decay of luminescence in inorganic phosphors: the case of Zn_2SiO_4:Mn, J. Chem. Phys. 74 (1981) 4347–4355, doi:10.1063/1.441677.

[22] W.F. Hornyak, R. Chen, Thermoluminescence and phosphorescence with a continuous, J. Lumin. 44 (1989).

[23] W.L. Medlin, Decay of phosphorescence from a distribution of trapping levels, Phys. Rev. 123 (1961) 502–509, doi:10.1103/PhysRev.123.502.

[24] E. Mihóková, M. Nikl, Luminescent materials: probing the excited state of emission centers by spectroscopic methods, Meas. Sci. Technol. 26 (2015), doi:10.1088/0957-0233/26/1/012001.

[25] J. Ueda, P. Dorenbos, A.J.J. Bos, A. Meijerink, S. Tanabe, Insight into the thermal quenching mechanism for $Y_3Al_5O_{12}$:Ce^{3+} through thermoluminescence excitation spectroscopy, J. Phys. Chem. C 119 (2015) 25003–25008, doi:10.1021/acs.jpcc.5b08828.

[26] A. Vedda, M. Martini, F. Meinardi, J. Chval, M. Dusek, J. Mares, E. Mihokova, M. Nikl, Tunneling process in thermally stimulated luminescence of mixed crystals, Phys. Rev. B Condens. Matter Mater. Phys. 61 (2000) 8081–8086, doi:10.1103/PhysRevB.61.8081.

[27] P. Bolek, D. Kulesza, A.J.J. Bos, E. Zych, The role of Ti in charge carriers trapping in the red-emitting Lu_2O_3:Pr,Ti phosphor, J. Lumin. 194 (2018) 641–648.

[28] P. Dorenbos, Modeling the chemical shift of lanthanide 4 f electron binding energies, Phys. Rev. B 85 (2012) 165107, doi:10.1103/PhysRevB.85.165107.

[29] P. Dorenbos, The electronic level structure of lanthanide impurities in REPO 4, REBO3, REAlO3, and RE2O 3 (RE = La, Gd, Y, Lu, Sc) compounds, J. Phys. Condens. Matter. 25 (2013), doi:10.1088/0953-8984/25/22/225501.

[30] P. Dorenbos, Charge transfer bands in optical materials and related defect level location, Opt. Mater. 69 (2017) 8–22 (Amst)., doi:10.1016/j.optmat.2017.03.061.

[31] P. Dorenbos, Improved parameters for the lanthanide 4fq and 4fq−15d curves in HRBE and VRBE schemes that takes the nephelauxetic effect into account, J. Lumin. 222 (2020) 0–10, doi:10.1016/j.jlumin.2020.117164.

[32] D. Van der Heggen, D. Vandenberghe, N.K. Moayed, J. De Grave, P.F. Smet, J.J. Joos, The almost hidden role of deep traps when measuring afterglow and thermoluminescence of persistent phosphors, J. Lumin. 226 (2020), doi:10.1016/j.jlumin.2020.117496.

[33] S.W.S. Mckeever, R. Chen, Luminescence models, Radiat. Meas. 27 (1997) 625–661, doi:10.1016/S1350-4487(97)00203-5.

[34] S.W.S. McKeever, Theoretical background, in: Thermoluminescence of Solids, Cambridge University Press, 1985, pp. 20–63, doi:10.1017/CBO9780511564994.003.

[35] J. Trojan-Piegza, E. Zych, J. Hölsä, J. Niittykoski, Spectroscopic properties of persistent luminescence phosphors : Lu_2O_3:Tb^{3+},M^{2+} (M= Ca, Sr, Ba), J. Phys. Chem. C 113 (2009) 20493–20498.